Article (refereed) - postprint

Jin, Shuqin; Zhang, Bin; Wu, Bi; Han, Dongmei; Hu, Yu; Ren, Chenchen; Zhang, Chuanzhen; Wei, Xun; Wu, Yan; Mol, Arthur P.J.; Reis, Stefan; Gu, Baojing; Chen, Jie. 2021. **Decoupling livestock and crop production at the household level in China**. *Nature Sustainability*, 4 (1). 48-55. https://doi.org/10.1038/s41893-020-00596-0

Title: Conservation slows down emission increase from a tropical peatland in Indonesia

Author list and affiliations

Chandra S. Deshmukh[1,*], Dony Julius[1], Ankur R. Desai[2], Adibtya Asyhari[1], Susan E. Page[3], Nardi[1], Ari P. Susanto[1], Nurholis[1], M. Hendrizal[1], Sofyan Kurnianto[1], Yogi Suardiwerianto[1], Yuandanis W. Salam[1], Fahmuddin Agus[4], Dwi Astiani[5], Supiandi Sabiham[6], Vincent Gauci[7], Chris D. Evans[8]

[1]Asia Pacific Resources International Ltd., Kabupaten Pelalawan, Indonesia

[2]Department of Atmospheric and Oceanic Sciences, University of Wisconsin-Madison, Madison, WI, USA

[3]Centre for Landscape and Climate Research, School of Geography, Geology and the Environment, University of Leicester, Leicester, UK

[4]Indonesian Center for Agricultural Land Resources Research and Development, Bogor, Indonesia

[5]Faculty of Forestry Universitas Tanjungpura, Jl Daya Nasional Pontianak, Indonesia

[6]Department of Soil Science and Land Resource, Institut Pertanian Bogor, Bogor, Indonesia

[7]Birmingham Institute of Forest Research (BIFoR) and School of Geography, Earth and Environmental Sciences, University of Birmingham, B15 2TT, UK

[8]Centre for Ecology and Hydrology, Bangor, UK

*Corresponding author: Chandra S. Deshmukh Chandra_Deshmukh@aprilasia.com

Abstract

Tropical peatlands are threatened by climate and land-use changes, but there remain substantial uncertainties about their present and future role in the global carbon cycle due to limited measurements. Here, we present measurements of CO_2 and CH_4 emissions between mid-2017 and mid-2020 as well as N_2O emissions between 2019 and 2020 at two contrasting sites in a coastal peatland in Sumatra, Indonesia. We find that greenhouse gas emissions from intact peatlands increased significantly due to an extreme drought caused by a positive Indian Ocean Dipole phase combined with El Niño. The emission in the degraded site was two times greater than at the intact site. The smaller emission in the intact peatland suggests that protecting the remaining intact tropical peatlands from degradation offers significant climate benefits, avoiding greenhouse gas emissions of 24 ± 5 tCO_2e ha^{-1} yr^{-1} (average ± standard deviation) at our study site in Indonesia.

Tropical peatlands have been one of the most important global sinks of atmospheric carbon dioxide (CO_2) over millennia and have accumulated at least 75 Gt carbon under anoxic water-logged conditions[1-6]. However, they are vulnerable to climate change[7-9], especially responses to the hydrologic cycle[10-13]. Thus, variability and change in rainfall regime are important factors determining peat carbon accumulation and loss[11-13]. Most tropical peatlands have formed since the Last Glacial Maximum[14-16]. In Southeast Asia, which holds one of the world's largest tropical peatland areas[5], the coastal peatlands were initiated following a sea level high-stand, coupled with ample year-round rainfall and low intensity and frequency of droughts[11,14-16]. In recent times, more frequent and severe El Niño–Southern Oscillation (ENSO)[17] and the linked positive phase of Indian Ocean Dipole

(IOD)[18] may change local hydrology in this region[19,20]. Increasing rainfall seasonality lowers dry season groundwater level (GWL) and permits oxidation of previously stored carbon[10-13]. Yet almost no high-quality contemporary CO_2 flux measurements exist for the remaining intact tropical peatlands in Southeast Asia. Previous research in Borneo[21,22] reported flux measurements from peatlands disturbed by historical forest cover loss due to selective logging and these data do not necessarily represent an intact reference. Given the role of intact tropical peatlands in long-term climate mitigation through carbon sequestration, an improved understanding of their fate under current and future climate is a prerequisite for assessing the significance of peatland conservation as a climate mitigation strategy[23,24].

Tropical peatlands are among the world's most threatened ecosystems due to land-cover changes driven by transmigration, population growth and ongoing economic development[25,26]. Large-scale artificial drainage exposes previously accumulated peat carbon to oxygen and promotes aerobic decomposition, resulting in CO_2 emissions and subsidence of the peatland surface[27,28].

In addition, tropical peatlands also emit methane (CH_4)[29] and nitrous oxide (N_2O)[30], potent greenhouse gases (GHGs)[31] which may be modified by land-cover change[29,30]. However, assessments of full GHGs budgets are scarce and CH_4 and N_2O contributions remain highly uncertain. Tropical peatlands are reported to be GHG sources[23] in the order of 1.48 $GtCO_2e\ yr^{-1}$, but with a wide uncertainty range of 0.04-2.79 $GtCO_2e\ yr^{-1}$, reflecting a lack of comprehensive quantitative understanding of emissions from these ecosystems. Given the sensitivity of peat GHG emissions to changes in hydrology and/or vegetation, we cannot adequately capture their global climate impact, manage peatlands responsibly or optimize mitigation measures if we do not know the scale of GHG emissions from tropical peatlands[32,33].

Here, we report on a paired of eddy covariance (EC) study that measured continuous net ecosystem CO_2, CH_4 and H_2O (evapotranspiration) exchanges for seven site-years over two land-cover types within the same peat landscape on the Kampar Peninsula in Sumatra, Indonesia: (1) an intact peatland and (2) a degraded peatland with disturbed hydrology and forest cover loss (Figure 1, Extended Data Table 1). Such comparative studies are rare for peatlands globally (see Methods for a detailed description). Soil N_2O fluxes from manual soil flux chamber measurements were also incorporated to obtain comprehensive GHG budgets. In addition, we also measured peat subsidence around the EC towers. Finally, we linked measured rainfall, evapotranspiration and GWL data to the GHG budget.

Significant CO_2 emissions from an intact peatland

During the study period, June 2017-May 2020, the average GWL was -0.27 ± 0.23 m (average ± standard deviation, negative sign indicates that the GWL was below the hollow peat surface). The intact peatland emitted 15.5 ± 8.8 $tCO_2\ ha^{-1}\ yr^{-1}$ and subsided 3.3 ± 0.7 $cm\ yr^{-1}$ (Table 1, Extended Data Table 2).

Net ecosystem CO_2 exchange showed a clear seasonal pattern corresponding to GWL fluctuation (Figure 2). GWL rose up to 0.19 m above the hollow peat surface and remained above the surface for only 16% of the study period. The intact peatland showed a monthly CO_2 uptake of 1.3 ± 0.4 $tCO_2\ ha^{-1}$ when the peat surface was inundated in January 2018 but a monthly CO_2 emission of 3.8 ± 0.7 $tCO_2\ ha^{-1}$ in October 2019 when GWL fell to 0.78

m below the hollow peat surface. GWL drawdown coincided with an extended dry season when a major positive IOD combined with an El Niño event. Over a 3-month period (July–September 2019), there was only 89 mm of rainfall (Figure 2a, Extended Data Figure 1). Such deep GWL was also observed in an undrained tropical peatland in Kalimantan during the 2015 El Niño event[13]. The results indicate that during the measurement period (which included years with and without El Niño and positive IOD, Extended Data Figure 1), large CO_2 emissions during the dry seasons were not entirely offset by relatively small CO_2 uptake during the wet seasons. The climate sensitivity of the ecosystem was also demonstrated by interannual variations in the strength of dry and wet seasons, which led to corresponding variations in the duration and rate of wet season CO_2 uptake and dry season CO_2 emissions (Figure 2c). Notably, during the extended dry season from July 2019 through February 2020, rainfall was less than half compared to the same period in previous years (676 vs. 1385 mm) but evapotranspiration remained relatively constant (1014 vs. 1046 mm), leading to almost five times lower GWL as compared to the previous years (-0.51 vs. -0.11 m). This comparatively low GWL resulted in four times more CO_2 emissions than in the previous years during the same months (19.9 vs. 5.7 tCO_2 ha^{-1}) (Figure 2c).

Observed net CO_2 emissions is driven by changes in ecosystem respiration (R_{eco}). R_{eco} had a negative relationship with GWL (a proxy that captures both oxygen and water availability controls on peat respiration) (Extended Data Figure 2) as also reported in previous studies[21]. The gross primary production (GPP), an indicator of photosynthetic capacity of the vegetation community, also appeared to decrease with GWL drawdown (Extended Data Figure 2c). Notably, the intact peatland showed higher light-use efficiency when GWL was above -0.2 m as compared to deeper GWL (Extended Data Figure 2d). In an intact tropical peatland[34], significantly higher root biomass in elevated mounds and shallow lateral rooting mean that approximately 83% of the total live root biomass lies within the top 0.25 m of peat layer. Thus, we surmise that when GWL falls below a critical depth, there is inadequate vertical recharge of near-surface peat layers through capillary rise owing to high air-filled porosity. This effect likely causes near-surface peat desiccation and reduces stomatal conductance[35], thereby reducing CO_2 uptake and slowing down the translocation of photosynthates between above- and belowground biomass[21]. This sequence of events suggests that peat swamp forests are not adapted to low GWL[36].

The results suggest that changes in rainfall regime play a central role in shaping the seasonal and interannual variability of intact tropical peatland hydrology (Figure 2a), and therefore the CO_2 budget (Figure 2c). The observed CO_2 emissions due to GWL drawdown in this study are consistent with previous studies in tropical peatlands where the carbon loss[11,13], reduction in peat accumulation rate[17,37] and a hiatus in peat genesis[16] have been reported in response to droughts driven by ENSO activity.

The relationship between net ecosystem CO_2 exchange and GWL suggests that the intact site would approach CO_2 neutrality if the peat hollow surfaces were continuously flooded (Figure 3a). Rainfall, evapotranspiration and GWL measurements clearly demonstrated that during the dry period the ecosystem's demand for evapotranspiration exceeded the rainfall in this ombrotrophic environment (Figure 2a). This resulted in GWL drawdown, even though the study area is hydrologically connected to a large peat dome. The condition was exacerbated during prolonged drought periods induced by climate extremes, for instance during the strong positive IOD together with El Nino event which occurred during 2019. This significantly low GWL driven by rainfall deficit can lead to tree mortality[36], CO_2 emissions[12] and subsidence in these ecosystems. The results indicate that the long-term rate of carbon accumulation of 2.8 tCO_2 ha^{-1} yr^{-1} in coastal peatlands of Indonesia[1] may no longer occur under current rainfall regime. This is further indicated by observed subsidence (3.1 cm yr^{-1}) at the sampling location far away from the forest edge (>5 km), that should have minor effects (if any) of regional land-cover change[38].

Observed net CO_2 emissions during years without El Niño and positive IOD events are more surprising, since an intact peatland would be expected to act as a long-term CO_2 sink. This may raise the possibility that chronic long-term changes in rainfall seasonality and quantity[8-10,] could be promoting a large-scale shift of the tropical peatland carbon balance, exacerbated by superimposed and/or lagged responses to periodic El Niño or positive IOD events. Longer term measurements from this and other sites are therefore needed to establish whether our observations are occurring across other remaining areas of intact peatland and to provide reliable and robust understanding of long-term climate responses.

Degradation enhances CO_2 emissions

During the study period, October 2016–September 2020, GWL in the degraded peatland ranged between -0.21 to -1.18 m with an average of -0.66 ± 0.21 m, indicating that a significant part of the peat profile was aerated throughout the year (Figure 2b). The degraded peatland emitted 39.8 ± 2.9 tCO_2 ha^{-1} yr^{-1} and subsided 4.2 ± 1.3 cm yr^{-1} (Table 1, Extended Data Table 2).

We attribute observed high R_{eco} at the degraded site to four interlinked ecosystem responses to degradation. Firstly, greater peat aeration due to consistently deeper GWL enhances heterotrophic respiration rates. Secondly, increased soil temperatures due to both canopy cover loss and GWL drawdown further boosts microbial activities and heterotrophic respiration (Extended Data Table 2). Thirdly, the area was noted to be continuously losing large trees from ‘edge-effect exposure’, where both wind exposure and deeper GWL are probably involved. Big trees are a dominant repository of above-ground carbon stock in tropical peatlands and even a modest rate of loss may exceed the biomass gain by any number of small trees. The contribution of CO_2 emissions from peat decomposition is experienced immediately after GWL drawdown, but the release of CO_2 from coarse woody debris may be delayed as dead trees do not decompose instantaneously, providing a lagged but sustained contribution to R_{eco}[39]. Finally, R_{eco} may be enhanced by higher autotrophic respiration as a result of higher GPP from regenerating trees and shrubs.

In contrast to the intact peatland, net ecosystem CO_2 exchange at the degraded peatland appeared to be less sensitive to GWL changes (Figure 3a). Net ecosystem CO_2 exchange did not change with GWL from -0.4 to -0.8 m at the degraded site as the increase in R_{eco} was fully offset by increased GPP (Extended Data Figure 2b,c). The adaptation of tree species to a low GWL environment has been reported in a drained tropical peatland[21]. Tree roots grow into aerated deeper peat layers and hence these trees do not experience water stress even with a GWL of -0.9 m[21]. However, the increase in GPP with deeper GWL may not sustain with further drawdown in the later part of a prolonged dry season when GWL falls below a critical level[21].

Emissions of CH_4, N_2O and fluvial carbon export

The intact peatland emitted 73 ± 31 $kgCH_4\ ha^{-1}\ yr^{-1}$ and 0.2 ± 0.2 $kgN_2O\ ha^{-1}\ yr^{-1}$ (Table 1). A proportion of ecosystem net primary production is also exported in the forms of dissolved inorganic/organic and particulate organic carbon via lateral export. A fluvial carbon export of 1.1 ± 0.2 $tC\ ha^{-1}\ yr^{-1}$ was reported in the intact peatland within the same landscape[40]. We conservatively assume that all fluvial carbon is ultimately emitted as CO_2[41]. Similarly, the degraded peatland emitted 43 ± 11 $kgCH_4\ ha^{-1}\ yr^{-1}$ and 1.1 ± 0.6 $kgN_2O\ ha^{-1}\ yr^{-1}$. A fluvial carbon export of 1.8 ± 0.4 $tC\ ha^{-1}\ yr^{-1}$ can further occur from a drained tropical peatland[40].

GWL is a key driver of CH_4 emissions from tropical peatlands[29] (Figure 3b). The lower GWL reduces CH_4 emissions as aerobic conditions are unfavorable to methanogens and promote methanotrophy. In addition, GWL drawdown below the root zone will limit plant-mediated transport of CH_4 from the anaerobic zone to the atmosphere[29]. Higher N_2O emissions at the degraded peatland as compared to the intact site can be due to accelerated mineralization of the peat under aerobic conditions, releasing mineral nitrogen as ammonium (Extended Data Table 1) and producing N_2O as a by-product of the nitrification process[42].

Climate benefits from tropical peatland conservation

Our study indicates that peatland degradation resulted in a significant increase in net CO_2 emissions, decrease in CH_4 emissions and increase in N_2O emissions (Table 1). We computed GHG balance of both sites using sustained-flux global warming potential of 1, 45 and 270 for CO_2, CH_4 and N_2O over a 100-year time period[43]. The GHG balance for

CO_2, CH_4 and N_2O increased from 20.0 ± 4.5 $tCO_2e\ ha^{-1}\ yr^{-1}$ at the intact site to 43.8 ± 1.5 $tCO_2e\ ha^{-1}\ yr^{-1}$ at the degraded site. Although the measurements indicate that both intact and degraded peatlands in this study are warming the atmosphere (Table 1), it remains clear that protection of the remaining intact tropical peatlands in Indonesia offers a viable way to avoid substantial GHG emissions from this globally important ecosystem. The results suggest that protecting intact tropical peatland in Sumatra from degradation effectively avoid GHG emissions of 23.8 ± 4.7 $tCO_2e\ ha^{-1}\ yr^{-1}$ (Table 1). The results highlight that conserving all remaining intact peat swamp forests in Sumatra and Kalimantan (5.97 Mha)[44] will avoid GHG emissions of around 0.14 $GtCO_2e\ yr^{-1}$. This equates to ~10% of Indonesia's GHG emissions in 2016. This estimate is conservative. If some remaining intact peatlands are continuing to sequester CO_2, the avoided emissions will be correspondingly higher. The Paris Agreement target to keep global warming to below 2.0°C above pre-industrial times reinforces REDD+ (Reducing Emissions from Deforestation and Forest Degradation). The role of conservation in the responsible management of peatland landscapes[33] in developing countries is a key component of future global climate change mitigation efforts. Apart from protecting carbon stock and avoiding GHG emissions, intact tropical peatlands deliver ecosystem services such as water storage, flood protection, nature-based recreation and biodiversity support. Given the rapid observed changes in rainfall regime and land-use, conservation measures implemented now will be more effective than those implemented in future, because any delay will likely lead to continued forest loss and ecosystem degradation, requiring greater restoration effort which will cost more[45] and be more challenging[46].

Therefore, peatland management approaches[33] that integrate evidence-based, long-term conservation commitment and finance should be encouraged.

The estimated effect of peatland degradation on GHG emissions related to land-cover change that we present here may vary in time and space. In addition to variations related to natural hydrology driven by rainfall, the effect is also likely to vary with degradation level[21] including forest cover loss and drainage intensity. Furthermore, results presented here are specific for coastal Indonesian peatlands, thus, should not be extrapolated to other tropical peatlands, such as those of the Amazon and Congo basins, since they have different rainfall regimes, vegetation and peat formation history. Therefore, more ecosystem-scale measurements from the peatlands within Amazon and Congo basins are needed since they are also of global significance in terms of future potential deforestation and degradation driven by both land-use and climatic changes[9,26,47].

A strong negative relationship between CO_2 emissions and GWL for peatlands across Southeast Asia (Extended Data Figure 3) suggests that our results may be regionally applicable. Over coming decades, it is likely that tropical peatland ecosystems will become increasingly exposed to changes in rainfall regime, such as those induced by more frequent and severe El Niño and positive IOD events[17,18]. The strong response of CO_2 emissions to extreme drought in the intact peatland site indicates the potential significance of climate regime in determining the future GHG budget of these ecosystems, highlighting their vulnerability and global consequences. Given the large GHG emissions, a continuing use of a long-term rate of carbon accumulation for future projection[7,24] is incompatible with ongoing efforts to better understand and manage remaining intact tropical peatlands in a changing climate and thus should be considered with caution. The results should help to reduce the uncertainty in the estimation of GHG budgets from a globally important ecosystem, develop science-based peatland management practices to reduce carbon emissions and improve the understanding of their role under current and future climate.

Reference

1. Dommain, R., Couwenberg, J. & Joosten, H. Development and carbon sequestration of tropical peat domes in south-east Asia: links to post-glacial sea-level changes and Holocene climate variability. *Quat. Sci. Rev.* **30**, 999–1010 (2011).
2. Dargie, G. C. et al. Age, extent and carbon storage of the central Congo Basin peatland complex. *Nature* **542**, 86–90 (2017).
3. Lähteenoja, O. et al. The large Amazonian peatland carbon sink in the subsiding Pastaza-Maranon foreland basin, Peru. *Glob. Change Biol.* **18**, 164-178 (2012).
4. Warren, M., Hergoualc'h, K., Kauffman, J. B., Murdiyarso, D., & Kolka, R. An appraisal of Indonesia's immense peat carbon stock using national peatland maps: uncertainties and potential losses from conversion. *Carbon Balance Manag.* **12(1)**, 12 (2017).
5. Gumbricht, T. et al. An expert system model for mapping tropical wetlands and peatlands reveals South America as the largest contributor. *Glob. Change Biol.* **36**, 335 (2017).
6. Xu, J., Morris, P. J., Liu, J., & Holden, J. PEATMAP: Refining estimates of global peatland distribution based on a meta-analysis. *Catena* **160**, 134–140 (2018).
7. Gallego-Sala, A. V. et al. Latitudinal limits to the predicted increase of the peatland carbon sink with warming. *Nat. Clim. Chan.* **8**, 907–913 (2018).

8. Loisel, J., et al. Expert assessment of future vulnerability of the global peatland carbon sink. *Nat. Clim. Chan*. **11**, 70–77 (2021).
9. Wang, S., Zhuang, Q., Lähteenoja, O., Draper, F. C. & Cadillo-Quiroz, H. Potential shift from a carbon sink to a source in Amazonian peatlands under a changing climate. *Proc. Natl. Acad. Sci.* **115**, 12407–12412 (2018).
10. Li, W. et al. Future precipitation changes and their implications for tropical peatlands. *Geophys. Res. Lett*. **34**, L01403 (2007).
11. Dommain, R., Couwenberg, J., Glaser, P. H., Joosten, H., & Suryadiputra, I. N. N. Carbon storage and release in Indonesian peatlands since the last deglaciation. *Quat. Sci. Rev*. **97**, 1–32 (2014).
12. Cobb, A. R. et al. How temporal patterns in rainfall determine the geomorphology and carbon fluxes of tropical peatlands. *Proc. Natl. Acad. Sci. USA* **114 (26)** E5187-E5196 (2017).
13. Swails, E. et al. The response of soil respiration to climatic drivers in undrained forest and drained oil palm plantations in an Indonesian peatland. *Biogeochemistry* **142**, 37–51 (2019).
14. Yu, Z., Loisel, J., Brosseau, D. P., Beilman, D. W., & Hunt, S. J. Global peatland dynamics since the last glacial maximum. *Geophys. Res. Lett*. **37**, L13402 (2010).
15. Morris, P. J. et al. Global peatland initiation driven by regionally asynchronous warming. *Proc. Natl. Acad. Sci. USA* **115**, 4851– 4856 (2018).
16. Ruwaimana, M. Anshari, G. Z. Silva, L. C. R. & Gavin, D. G. The oldest extant tropical peatland in the world: a major carbon reservoir for at least 47,000 years. *Environ. Res. Lett*. 15 (2020).

17. Cai, W. et al. Increasing frequency of extreme El Niño events due to greenhouse warming. *Nat. Clim. Chan.* **4**, 111–116 (2014).
18. Cai, W. et al. Increased frequency of extreme Indian Ocean Dipole events due to greenhouse warming. *Nature* **510**, 254–258 (2014).
19. Saji, N.H., Goswami, B.N., Vinayachandran, P.N., & Yamagata, T. A dipole mode in the tropical Indian Ocean. *Nature* **401**, 360-363 (1999).
20. Alsepan, G., & Minobe, S. Relations between interannual variability of regional-scale Indonesian precipitation and large-scale climate dodes during 1960–2007. *J. Climate* **33**, 5271–5291 (2020).
21. Hirano, T., et al. Effects of disturbances on the carbon balance of tropical peat swamp forests. *Glob. Change Biol.* **18**, 3410–3422 (2012).
22. Tang, A. C., et al. A Bornean peat swamp forest is a net source of carbon dioxide to the atmosphere. *Glob Change Biol*. **26(12)**, 6931–6944 (2020).
23. Leifeld, J. & Menichetti, L. The underappreciated potential of peatlands in global climate change mitigation strategies. *Nat. Commun.* **9**, 1–8 (2018).
24. Leifeld, J., Wüst-Galley, C., & Page, S. Intact and managed peatland soils as a source and sink of GHGs from 1850 to 2100. *Nat. Clim. Chan.* **9**, 1–3 (2019).
25. Miettinen, J., Shi, C., & Liew, S.C. Land-cover distribution in the peatlands of Peninsular Malaysia, Sumatra and Borneo in 2015 with changes since 1990. *Glob. Ecol. Conserv.* **6**, 67–78 (2016).
26. Roucoux, K. H. et al. Threats to intact tropical peatlands and opportunities for their conservation. *Conserv. Biol.* **31(6)**:1283–1292 (2017).

27. Hooijer, A. et al. Subsidence and carbon loss in drained tropical peatlands. *Biogeosciences* **9**, 1053–71 (2012).
28. Hoyt, A. M., Chaussard, E., Seppalainen, S. S. & Harvey C. F. Widespread subsidence and carbon emissions across Southeast Asian peatlands. *Nat. Geosci.* **13**, 435–440 (2020).
29. Deshmukh, C. S. et al. Impact of forest plantation on methane emissions from tropical peatland. *Glob. Change Biol.* **26,** 2477–2495 (2020).
30. Prananto, J. A., Minasny, B., Comeau, L-P., Rudiyanto, R., & Grace, P. Drainage increases CO_2 and N_2O emissions from tropical peat soils. *Glob Change Biol*. **00**:1–18 (2020).
31. Myhre, G. et al. In Climate Change 2013 (eds Stocker, T. F. et al.) 659–740 Cambridge University Press, Cambridge, UK and New York, USA, (2013).
32. Murdiyarso, D., Lilleskov, E. & Kolka, R. Tropical peatlands under siege: the need for evidence-based policies and strategies. *Mitig. Adapt. Strateg. Glob. Change* **24**, 493–505 (2019).
33. Clarke, D. & Rieley, J. O. Strategy for responsible peatland management. 6 Edition, International Peatland Society, Jyväskylä, Finland (2019).
34. Sulistiyanto, Y. Nutrient dynamics in different sub-types of peat swamp forest in Central Kalimantan, Indonesia. Doctoral dissertation, University of Nottingham. 225p. (2004).
35. Hirano, T., Kusin, K. Limin, S. & Osaki M. Evapotranspiration of tropical peat swamp forests. *Glob. Change Biol.* **21**, 1914–1927 (2015).

36. Nishimua, T. et al. Mortality and growth of trees in peat-swamp and heath forests in Central Kalimantan after severe drought. *Plant Ecol*. **188,** 165–177 (2007).
37. Kelly, T. J. et al. The vegetation history of an Amazonian domed peatland. *Palaeogeogr. Palaeoclimatol. Palaeoecol.* **468**, 129–141 (2017).
38. Cobb, A. R., Dommain, R. R., Tan, F., Heng, N. H. E., & Harvey, C. F. Carbon storage capacity of tropical peatlands in natural and artificial drainage networks. *Environ. Res. Lett*. **15**, 23–25 (2020).
39. Kiew, F. et al. Carbon dioxide balance of an oil palm plantation established on tropical peat. *Agric. For. Meteorol.* **295**, 1-8 (2020).
40. Yupi, H. M., Inoue, T., Bathgate, J., & Putra, R. Concentrations, loads and yields of organic carbon from two tropical peat swamp forest streams in Riau Province, Sumatra, Indonesia. *Mires and Peat*, **18**, 1–15 (2016).
41. Evans, C. D., Renou-Wilson, F. & Strack, M. The role of waterborne carbon in the greenhouse gas balance of drained and re-wetted peatlands. *Aquat Sci.* **78**, 573–590 (2016).
42. Jauhiainen, J. et al. Nitrous oxide fluxes from tropical peat with different disturbance history and management. *Biogeosciences* **9**, 1337–1350 (2012).
43. Neubauer, S. C., & Megonigal J. P. Moving beyond global warming potentials to quantify the climatic role of ecosystems. *Ecosystems* **18,** 1000–1013 (2015).
44. Wijedasa, L. S. et al. Carbon emissions from South-East Asian peatlands will increase despite emissionreduction schemes. *Glob. Change Biol.* **00**, 1–16 (2018).
45. Hansson, A. & Dargusch, P. An estimate of the financial cost of peatland restoration in Indonesia. *Case Stud. Environ.* **2(1)** 1–8 (2017).

46. Ward, C. et al. Wading through the swamp: what does tropical peatland restoration mean to national-level stakeholders in Indonesia? *Restor. Ecol.* **28**, 817-827 (2020).

47. Lilleskov, E. et al. Is Indonesian peatland loss a cautionary tale for Peru? A two-country comparison of the magnitude and causes of tropical peatland degradation. *Mitig. Adapt. Strateg. Glob. Change* **24**, 591–623 (2019).

ACKNOWLEDGEMENTS

The establishment and operation of the eddy covariance towers and associated data collection were funded by Asia Pacific Resources International Ltd (APRIL) and Riau Ecosystem Restoration (RER).

AUTHORS' CONTRIBUTIONS

C.S.D., C.D.E. and S.E.P. conceived of the study. C.S.D., D.J., A.P.S, Y.W.S, and A.R.D. completed eddy covariance data processing. D.J., Nardi, A.P.S., Nurholis, M.H., C.S.D., S.K., Y.S. and A.A. performed data collection, eddy covariance instruments calibration and maintenance. C.S.D. conceived the paper and wrote the initial draft, to which all authors provided critical contributions and approved submission.

CONFLICT OF INTEREST

C.D.E., S.E.P., S.S., V.G., F.A., and D.A. contributed to this paper as part of their contribution to the Independent Peat Expert Working Group (IPEWG), which was set up by Asia Pacific Resources International Ltd. (APRIL) to provide objective science-based advice on peatland management. ARD's contribution was also supported by APRIL to provide technical guidance on the Eddy Covariance data processing including quality controls and gap-filling protocols. C.S.D., D.J., Nardi, A.P.S., Nurholis, M.H., S.K., Y.S., A.A. and Y.W.S. are employed by APRIL to conduct data collection, instrument maintenance and calibration. The funders had no role in the interpretation of data, in the writing of the manuscript, or in the decision to publish the results. The authors declare that all views expressed are their own.

DATA AVAILABILITY STATEMENT

All data that support the findings of this study are archived on http://doi.org/10.5281/zenodo.4835696.

Methods

Study area

The study area, Kampar Peninsula, is an ombrotrophic coastal tropical peatland of around 700,000 ha and largely formed within the past 8,000 years[1]. The peat thickens from approximately 3 m deep near the river boundaries to over 11 m in the center of the approximately 60 km wide dome, with an average depth of 8 m. The peninsula experiences a humid tropical climate (warm year-round) with average monthly air temperature ranging from 26 to 28°C (Extended Data Table 2). The interannual variability of rainfall is influenced by ENSO and IOD[19,20] (Extended Data Figure 1). The average annual rainfall for the last 6 years (2014–2019, with 2015 El Niño, 2017 La Niña, and 2019 with a major positive IOD combined with an El Niño event) is ~1900 mm and characterized by a high seasonal variability with two rainfall peaks, one in November-December and one in March-April. The peninsula land-cover is characterized by a large central intact forest area surrounded by a mosaic of degraded peat swamp forest, industrial fiber wood plantation (largely *Acacia crassicarpa*), smallholder agriculture (largely oil palm, *Elaeis guineensis*) and degraded, shrub and undeveloped open land[25] (Figure 1).

The site selection for the intact peatland were carefully under taken to minimize any local land-use effect on measured fluxes. The intact peatland site is characterized as peat swamp forest[25,44] and comprises one of the largest remaining peat swamp forest in Southeast Asia. The forest structure was determined from vegetation survey in permanent sampling plots (20 x 125 m) around the tower. It was identified as mixed forest with uneven canopy (the tallest canopy is in a range of 28–35 m). Tree density with diameter at breast height >5 cm was 1,343 trees per hectare. The dominant tree species of the overstory are *Shorea uliginosa*, *Calophyllum ferrugineum* and *Syzygium spp.*; together they represent around 75% of the overstory vegetation (Extended Data Table 1). The understory is dominated by *Pandanus spp., Cyrtostachys renda* and *Nepenthes spp.* The forest floor is uneven with a hummock-hollow microtopography, and covered with tree debris, root mat and leaf litter. Hollow surfaces are often 20–40 cm lower than hummock tops. The average area ratio of hollow to hummock was 3:1 around the tower. The surface peat type is fibric and the average peat thickness is ~9.0 ± 1.0 m in the area surrounding the tower measured using the Eijkelkamp Peat Auger. The peat is composed almost entirely of organic matter with soil organic carbon of 50 ± 2% determined using the Loss on Ignition method and a dry bulk density of 0.08 ± 0.03 g cm^{-3} measured using the gravimetric method. These carbon concentration and dry bulk density values are consistent with other measurements in the region[48] (bulk density of 0.08 g cm^{-3} (0.07–0.09 g cm^{-3}) and carbon concentrations of 55% (53–57%)). The GWL fluctuates seasonally following the rainfall variation due to the ombrotrophic nature of the area[29]. An integrated climatologic footprint analysis[49] indicated that approximately 80% of fluxes were derived within one km in the upwind direction (Figure 1), and thus originated within intact peat swamp forest[25,44]. The area outside the flux footprint on the southeastern side of the tower site was disturbed somewhat by historic logging activity within the wider peat landscape in the 1990s, which included logging track and canal construction, or to the effects of plantation operation around the edge of the Kampar peat dome. While we cannot exclude some long-term hydrological effect of land use activities beyond the flux tower footprint on the study area, any such effects appear minor, and there is no indication that it has affected the functioning of the forest[25,44]. The closest logging track was more than 1 km from the flux tower site in the southeast direction and outside the flux measurement footprint. There was neither logging nor canal construction activity within the footprint and it retained an intact forest. The closest area of active plantation was 3.5 km to the southeast, well outside the flux footprint. To avoid any possible boundary effect and associated bias, the measurements between 78 and 191° wind direction were further excluded in this study (Figure 1).

The second tower is located on the boundary of plantation and degraded forest (Figure 1). To represent only the degraded area, the measurements between 270 and 90° wind direction were considered in this study. The degraded peatland was selectively logged and drained in the late 1990s and early 2000s, while some parts were burnt in 2014. The average canopy height was about 19 m (Extended Data Table 1). Tree densities with diameter at breast height >5 cm were 663 trees per hectare. Compared to the intact peatland site, more than 50% of the large trees have been logged or fallen and many of those remaining are now leaning. The dominant tree species of the over-story are *Syzygium claviflorum, Shorea teysmanniana, Stemonurus secundiflorus, Blumeodendron kurzii, Horsfieldia crassifolia* and *Macaranga pruinosa*; together they represent around 60% of the overstory vegetation. The understory is dominated by *Dicranopteris linearis*, *Nepenthes spp., Pandanus sp.* and *Cyrtostachys renda*. Formerly burned areas comprise of modest biomass in shrub, sedge and fern (*Nephrolepis sp., Stenochlaena sp.*, *Blechnum sp.*), with increasing cover of shrubs and small trees of *Macaranga pruinosa* with time since fire. The surface peat type is fibric and the average peat thickness is 8.2 ± 0.8 m. The forest floor in the degraded part was uneven with a hummock-hollow microtopography. Hummocks were relatively small in size (typically ~30 cm in height). The average area ratio of hollow to hummock was 3:1. There were no hummocks on the ground in the ex-burnt area. The surface peat is composed almost entirely of organic matter with soil organic carbon of 55 ± 0.5% and a dry bulk density of 0.09 ± 0.03 g cm^{-3}. The integrated climatologic footprint analysis[49] indicated that approximately 80% of fluxes originated within one km in the upwind direction and the ex-burnt area only represented 5% of the flux footprint (Figure 1). The average footprint can be considered as representative of the majority of unmanaged degraded peatlands in Southeast Asia[25].

The terrain around the towers is flat (slope <0.05%), ensuring a good fetch regardless of wind direction. The relatively close proximity of the intact peatland and the degraded peatland sites (~35 km apart) within the same peat landscape avoids potentially confounding variables such as climatic differences[1], past natural succession[50] and peat formation[51] (Figure 1, Extended Data Table 1). Thus, although it is inherently difficult and expensive to replicate flux measurements using the eddy covariance (EC) technique, the sites should provide a robust and unbiased basis for evaluating the effect of land-cover change (from intact peatland to degraded peatland) on CO_2 and CH_4 exchanges.

Eddy covariance and environmental variables measurements

The EC measurements were conducted for seven site-years (October 2016-September 2020 over the degraded site and June 2017-May 2020 over the intact site). The EC system consisted of an enclosed path CO_2/H_2O analyzer (LI-7200, LI-COR Inc.) to measure the atmospheric CO_2 and H_2O, an open path CH_4 analyzer (LI-7700, LI-COR Inc.) to measure CH_4 and a three-dimensional sonic anemometer (WindMaster Pro3-Axis Anemometer, Gill Instruments Limited) to measure orthogonal components of wind speed fluctuations. The sensors were mounted at the top of the tower to ensure complete exposure in all directions (Figure 1b,c). The raw turbulence EC data were recorded at 10 Hz using an analyzer interface unit (LI-7550, LI-COR Inc.) and stored on a removable flash disk (APRO, Industrial Grade USB Flash Disk). The filters of the CO_2 analyzer were manually cleaned either at biweekly or if the flow drive (indicating filter clogging condition) increased above 80% (LI-7200, LI-COR Inc.). The mirrors of the CH_4 analyzer were self-cleaned either at 5:00 (local time) every day or if the received signal strength indicator (RSSI) dropped below 20%. Furthermore, the upper and lower mirrors of the CH_4 analyzer were manually cleaned on a biweekly basis[29].

Quantum sensors (LI-190SL-50, LI-COR Inc.) were mounted at the top of the towers to measure the incoming photosynthetic photon flux density (PPFD, μmol m^{-2} s^{-1}). The vertical profiles of relative humidity (%) and air temperature (°C) were measured using air temperature and humidity probes (Vaisala HMP155 Humidity Temperature Probe, Vaisala Inc.), which were installed inside a ventilated radiation shield at five heights of 3, 7, 14, 21 and 40 m for the degraded site and 4, 11, 20, 29 and 48 m for the intact site. The vertical profiles of CO_2 concentrations were measured at four heights of 3, 14, 21 and 40 m for the degraded site and 4, 11, 29 and 48 m for the intact site to calculate flux storage term below the measurement height[21] using a closed-path CO_2 analyzer (LI-8100, LI-COR Inc.). The sampling lines were changed in rotation every 90 seconds and CO_2 concentrations were measured for last 10 seconds of each 90 seconds sampling time at each sampling height and recorded with a data logger (LI-8100, LI-COR Inc.); therefore, one rotation of measurements took six minutes in every 30 minutes. Both enclosed-path and closed-path CO_2 analyzers were calibrated every three months using ultra high-purity nitrogen as the zero-point gas for CO_2 and reference gases with concentration of 396 ppm CO_2 in air (certified grade ±1 ppm). Soil temperature (°C) was measured at 0.15 m below the hollow peat surface using temperature probe (Stevens Hydra Probe II, Stevens Water Monitoring Systems, Inc.) with three replicates at the intact peatland. The soil temperature were not measured at the degraded site due to the site logistic issues.

All meteorological sensors took measurements every second and were recorded as one minute average with a data logger (Sutron Model 9210 XLITE, Sutron Corporation). All measuring systems were powered using solar panels along with a rechargeable battery system (65 Watt Solar Package, SunWize Power & Battery).

Daily rainfall (mm d^{-1}) were measured using three and two manual bucket rain gauges within 11 km distance from the tower location in the intact site and the degraded site, respectively. Rain gauges were installed 1.5 m above the ground, in an open area so that rainfall was not intercepted by the tree canopy.

Peat subsidence was measured at eight locations in the intact site and four locations in the degraded site (Figure 1f,g), with hollow, perforated 5 cm diameter hollow polyvinyl chloride (PVC) poles, inserted vertically into the peat and anchored into underlying mineral subsoil following the approach described in ref[52]. Annual average subsidence rates were derived from measurements between December 2016-September 2020 and December 2017-June 2020 in the intact and the degraded peatland respectively.

GWLs (m) were monitored as the water elevation relative to the ground surface, taking the base of the hollows as a datum[29], every 30 min using GWL logger (Solinst Levelogger Model 3001). The three and two GWL loggers respectively at the intact and the degraded peatland were placed in a perforated PVC tubes that were inserted vertically into the peat around the towers (Figure 1f,g). The GWL logger also recorded temperature at 1.5 m below the peat surface. Additional GWLs were recorded biweekly at two locations per tower site and on a quarterly basis at additional four locations in transect in the intact peatland (Figure 1). Average GWLs were derived from nine and four monitoring locations in the intact peatland and the degraded peatland respectively.

Measured environmental variables are summarized in Extended Data Table 2 and presented in Extended Data Figure 5-6.

Eddy covariance data processing

Eddy covariance CO_2, CH_4 and H_2O (evapotranspiration) fluxes were computed from the 10 Hz concentration and vertical wind velocity data using EddyPro software (version 6.2.0, LI-COR Inc.) at a standard averaging interval of half-hour period[53]. A de-spiking procedure was applied to detect and eliminate individual out-of-range values for vertical wind velocity and concentrations[54]. De-trending was carried out using the block averaging method. A coordinate correction was applied to force the average vertical wind velocity to zero by the planar fit method[55]. Frequency response loss corrections were applied to compensate the flux losses at low and high frequencies[56]. The Webb-Pearman-Leuning correction[57] for air density fluctuations induced by temperature (thermal expansion) and water vapor (dilution) was applied. Differences between deployment specific variables, that is, sensor separation distance and instrument placement, were considered while processing the data. The half-hourly CO_2 storage below the flux measurement height was calculated from the four-point vertical profiles of CO_2 concentration, relative humidity and air temperature by temporal interpolation[21]. Finally, the net ecosystem CO_2 exchange was calculated as the sum of storage flux and eddy covariance flux. Owing to the large power requirement and cost of a separate CH_4 analyzer, we could not conduct CH_4 profile measurements to calculate CH_4 storage[29]. In theory, accumulated CH_4 below the canopy during nighttime is likely to be released and measured by the EC system following the onset of turbulence after sunrise and the bias on annual sums should be negligible[58]. We adopted the standard meteorological notation whereby a negative value denotes a net uptake of atmospheric CO_2 or CH_4 by the ecosystem, while a positive value indicates a net release of CO_2 or CH_4 from the ecosystem to the atmosphere[53].

After a set of quality controls[59-61] and system malfunctions due to lightning strikes and power supply failure, the numbers of high-quality measurements during the course of the study were 41% and 38% for CO_2, 32% and 26% for CH_4 and 34% and 33% for evapotranspiration in the intact and the degraded site, respectively. The similar range of 25-50% were reported for other tropical forested peatlands[21,29,35,39]. We considered a total half-hourly measurements of 12,926 and 10,694 for CO_2, 11,761 and 9,019 for CH_4 and 9,954 and 10,538 for evapotranspiration that met all quality criteria for the intact (between 191-78° wind direction) and the degraded (between 270-90° wind direction) site, respectively. We gap-filled both low-quality and missing data, as is commonly done in eddy covariance studies[21,29,35,39,62-67].

For CO_2, we applied three gap-filling approaches (a) marginal distribution sampling (MDS)[21,63], (b) artificial neural network (ANN)[65]; and (c) random forest (RF)[66]. In addition, we applied principal component analysis as an input to the algorithms to address multidriver dependency of CO_2 exchange and reduce the internal complexity of the algorithmic structures for the MDS approach[67]. Following other regional eddy covariance studies in peat swamp forests[21], we performed MDS gap-filling using the REddyProc package on a half-hourly basis[68] separately for the daytime (0600-1800 hr) and the nighttime (1800-0600 hr) data. ANN and RF procedures were iterated 20 times. Average of the 20 models were used to fill the gap and standard deviation was used to quantify uncertainty due to gap-filling. Nighttime CO_2 exchanges were considered equivalent to ecosystem respiration (R_{eco})[69]. PPFD, VPD, T_{air}, GWL and friction velocity were used for the daytime, and PPFD and VPD were excluded in the nighttime. GWL is reported as the main controlling factor of R_{eco} from tropical peatlands[21]. Therefore, we used GWL as environmental factors for the look-up table to derive daytime R_{eco} using the MDS gap-filling algorithm[68]. Then, GPP was calculated as the difference between CO_2 exchange and R_{eco} on a half-hourly basis[69]. Negative GPP represent gross CO_2 uptake by the ecosystem whereas positive R_{eco} represent the gross CO_2 release from the ecosystem to the atmosphere[53]. We applied the same above gap-filling approaches for evapotranspiration, using net radiation instead of PPFD during daytime, while adding net radiation and VPD during nighttime. To provide a conservative estimate of CO_2 and evapotranspiration, we used the average of the three approaches (Extended Data Table 3). After gap-filling, we corrected daily evapotranspiration for the energy imbalance using net radiation, sensible heat and latent heat as described in ref[35]. We applied two gap-filling approaches, mean diurnal course (MDC) and MDS, for CH_4 as described in ref[29]. To provide a conservative estimate of CH_4, we used the average of the MDC and MDS approaches (Extended Data Table 3).

Flux random uncertainty was calculated following ref[70]. The standard deviation of three different flux values derived from friction velocity thresholds of 5th, 50th and 95th percentiles were applied as an uncertainty due to friction velocity threshold using the REddyProc package[68]. The total uncertainty in CO_2, CH_4 and evapotranspiration (Extended Data Table 3) was calculated with the law of propagation of errors[71].

Soil N_2O flux measurements

Soil N_2O fluxes were measured using the manual soil flux chamber[72] within 2 km from the EC towers. Three and four plots were selected in the intact and degraded peatland, respectively (Figure 1f,g). At each plots, two stainless steel rectangular collars (surface area of 0.08 m^2) on hummocks and four in the adjacent hollow (randomly around 50-100 m apart) were inserted permanently 5 cm into the soil five months before the flux sampling was started. Within 45 min, four air samples (in duplicates) from the chamber were collected with a syringe and needle at 15 min intervals starting from the initial time when chambers were placed onto the collars. The air within the chambers was gently mixed prior to sample extraction using the syringe and needle. Air samples were transferred into pre-evacuated 20 ml glass vials capped with butyl stoppers and aluminum seals. Analysis of N_2O concentration was performed by gas chromatography (SRI® 8610C gas chromatograph, USA) equipped with an electron capture detector within 48 hours. Commercial gas standards with concentration of 350 ppbv N_2O in N_2 (uncertainties less than 10%) were injected after an analysis of every 10 samples for calibration. Nitrous oxide fluxes were calculated applying the ideal gas law to the slope of the linear regression of gas concentration in the chamber versus time. The soil N_2O flux measurements were made during the dry and wet season to represent variation in the GWL and soil temperature. We averaged the soil N_2O fluxes of all replicates from each sampling month, then we averaged all monthly values (June 2019-December 2020 for the intact and July 2019-December 2020 for the degraded peatland) to estimate annual N_2O emissions. Thus our annual estimates cover both spatial and temporal variability. We didn't measure emissions from tree stems, this inclusion may increase total annual N_2O emissions by 11-38%[73]. Notably, given a minor (<1%) contribution of N_2O to total GHG balance, our reported GHG emissions should be considered representative.

References

48. Couwenberg, J. & Hooijer, A. Towards robust subsidence-based soil carbon emission factors for peat soils in south-east Asia, with special reference to oil palm plantations. *Mires Peat* **12**, 1 (2013).
49. Kljun, N., Calanca, P., Rotach, M. W., & Schmid, H. P. A simple two-dimensional parameterisation for Flux Footprint Prediction (FFP). *Geosci. Model Dev.* **8**, 3695–3713 (2015).

50. Cole, L. E. S., Bhagwat, S. A., & Willis, K. J. Long-term disturbance dynamics and resilience of tropical peat swamp forests. *J. Ecol.* **103**, 16–30 (2015)
51. Hapsari, K. A. et al. Environmental dynamics and carbon accumulation rate of a tropical peatland in Central Sumatra, Indonesia. *Quat. Sci. Rev*. **169**, 173–187 (2017).
52. Evans, C. D. et al. Rates and spatial variability of peat subsidence in Acacia plantation and forest landscapes in Sumatra, Indonesia. *Geoderma* **338**, 410–421 (2019).
53. Aubinet, M. et al. Estimates of the annual net carbon and water exchange of European forests: The EUROFLUX methodology. *Adv. Ecol. Res.* **30**, 113–175 (2000).
54. Vickers, D., & Mahrt, L. Quality control and flux sampling problems for tower and aircraft data. J. *Atmos. Oceanic Technol.* **14,** 512–526 (1997).
55. Wilczak, J. M., Oncley, S. P., & Stage, S. A. Sonic anemometer tilt correction algorithms. *Bound.-Layer Meteorol.* **99,** 127–150 (2001).
56. Massman, W. J. A simple method for estimating frequency response corrections for eddy covariance systems. *Agric. For. Meteorol.* **104(3)**, 185–198 (2000).
57. Webb, E. K., Pearman, G. I., & Leuning, R. Correction of flux measurements for density effects due to heat andwater vapour transfer. Q*. J. R. Meteorol. Soc.* **106**, 85–100 (1980).
58. Xu, K. E., et al. The eddy-covariance storage term in air: Consistent community resources improve flux measurement reliability. *Agric. For. Meteorol.* **279**, 107734 (2019).

59. Foken, T., & Wichura B. Tools for quality assessment of surface-based flux measurements. *Agric. For. Meteorol.* **78**, 83–105 (1996).

60. Mauder, M. et al. A strategy for quality and uncertainty assessment of long-term eddy-covariance measurements. *Agric. For. Meteorol.* **169**, 122–135 (2013).

61. Papale, D. et al. Towards a standardized processing of net ecosystem exchange measured with eddy covariance technique: algorithms and uncertainty estimation. *Biogeosciences* **3**, 571–583 (2006).

62. Falge, E. et al. Gap-filling strategies for defensible annual sums of net ecosystem exchange. *Agric. For. Meteorol.* **107(1)**, 43–69 (2001).

63. Kiew, F., et al. CO_2 balance of a secondary tropical peat swamp forest in Sarawak, Malaysia. *Agr. For. Meteorol*. **248**, 494–501 (2018).

64. Moffat, A. M. et al. Comprehensive comparison of gap-filling techniques for eddy covariance net carbon fluxes. *Agric. For. Meteorol.* **147(3)**, 209–232 (2007)

65. Papale, D., & Valentini, R. A new assessment of European forests carbon exchanges by eddy fluxes and artificial neural network spatialization. *Glob. Change Biol.* **9(4)**, 525–535 (2003).

66. Xu, T. et al. Evaluating different machine learning methods for upscaling evapotranspiration from flux towers to the regional scale. *J. Geophys. Res. Atmos.* **123(16)**, 8674–8690 (2018).

67. Kim, Y. et al. Gap-filling approaches for eddy covariance methane fluxes: A comparison of three machine learning algorithms and a traditional method with principal component analysis. *Glob. Change Biol.* **00:**1–20 (2019).

68. Wutzler, T. et al. Basic and extensible post-processing of eddy covariance flux data with REddyProc. *Biogeosciences* **15**, 5015–5030 (2018).

69. Reichstein, M. et al. On the separation of net ecosystem exchange into assimilation and ecosystem respiration: review and improved algorithm. *Glob. Change Biol.* **11**, 1424–1439 (2005).

70. Finkelstein, P. L., & Sims, P. F. Sampling error in eddy correlation flux measurements. *J. Geophys. Res.* **106(D4)**, 3503–3509 (2001).

71. Deventer, M. J. et al. Error characterization of methane fluxes and budgets derived from a long-term comparison of open- and closed-path eddy covariance systems. *Agric. For. Meteorol.* **278**, 107638 (2019).

72. Serça, D., Delmas, R., Jambert, C. & Labroue, L. Emissions of nitrogen oxides from equatorial rain forest in central Africa: origin and regulation of NO emission from soils. *Tellus* **46B,** 243-254 (1994).

73. Iddris, N. A.-A., Corre, M. D., Yemefack, M., van Straaten, O., & Veldkamp, E. Stem and soil nitrous oxide fluxes from rainforest and cacao agroforest on highly weathered soils in the Congo Basin. *Biogeosciences,* **17**, 5377–5397 (2020).

692 Table 1 | Greenhouse gas balance (average ± standard deviation) at the intact peatland and the degraded peatland in Sumatra, Indonesia. To quantify GHG balance in CO_2-equivalent, we used sustained-flux global warming potential of 1, 45 and 270 for CO_2, CH_4 and N_2O over a 100-year time period, respectively[43]. We assumed that all fluvial carbon export is ultimately converted to CO_2[41]. Change in GHG balance due to peatland degradation in Sumatra is given in lowermost line.

	Intact peatland	Degraded peatland
Net ecosystem CO_2 exchange (tCO_2 ha^{-1} yr^{-1})	15.5 ± 8.8	39.8 ± 2.9
Net ecosystem CH_4 exchange ($kgCH_4$ ha^{-1} yr^{-1})	73 ± 31	43 ± 11
Soil N_2O flux (kgN_2O ha^{-1} yr^{-1})	0.2 ± 0.2	1.1 ± 0.6
Fluvial carbon export (tC ha^{-1} yr^{-1})	0.3 ± 0.1	0.5 ± 0.1
GHG balance (tCO_2e ha^{-1} yr^{-1})		
CO_2	15.5 ± 8.8	39.8 ± 2.9
CH_4	3.3 ± 1.4	1.9 ± 0.5
N_2O	0.1 ± 0.1	0.3 ± 0.2
Fluvial carbon export	1.1 ± 0.2	1.8 ± 0.4
Total	20.0 ± 4.5	43.8 ± 1.5
Change in GHG balance due to peatland degradation (tCO_2e ha^{-1} yr^{-1})		23.8 ± 4.7

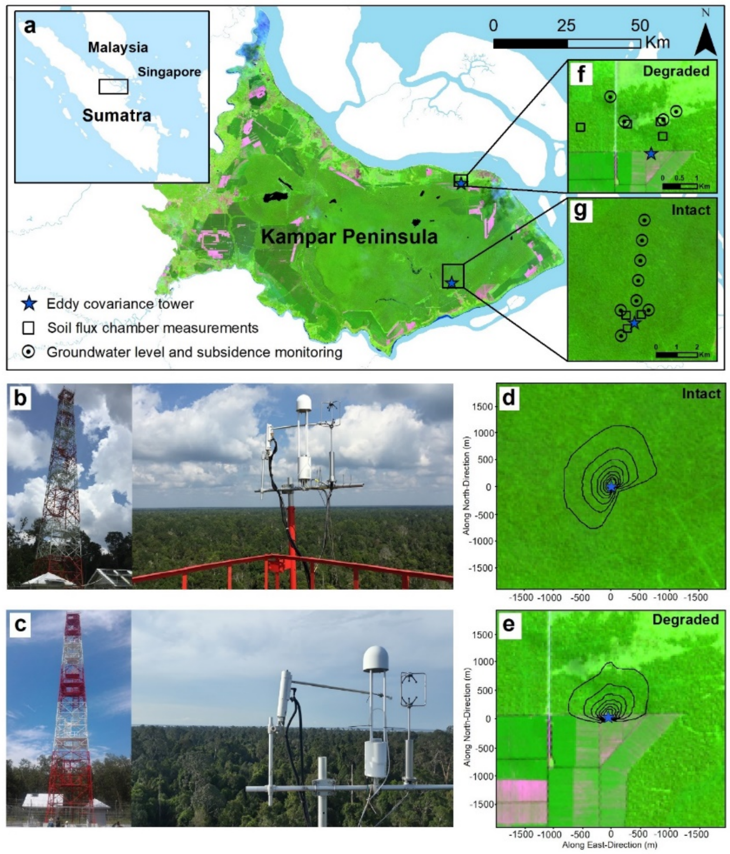

Figure 1 | Location of study area, Kampar Peninsula, Sumatra, Indonesia. (a) The location of research eddy covariance tower sites with satellite image taken from Landsat 8 (Source: https://earthexplorer.usgs.gov/). Photographs of the eddy covariance instruments installed at the top of the tower at (b) the intact peatland and (c) the degraded peatland. Integrated eddy covariance footprint contour lines from 10% to 80% in 10% intervals over (d) the intact peatland for June 2017–May 2020 and (e) the degraded peatland for October 2016–September 2020. Groundwater level, peat subsidence and soil nitrous oxide flux measurement locations at (f) the degraded peatland and (g) the intact peatland. An integrated climatologic footprint analysis indicated that approximately 80% of fluxes were derived within one km in the upwind direction.

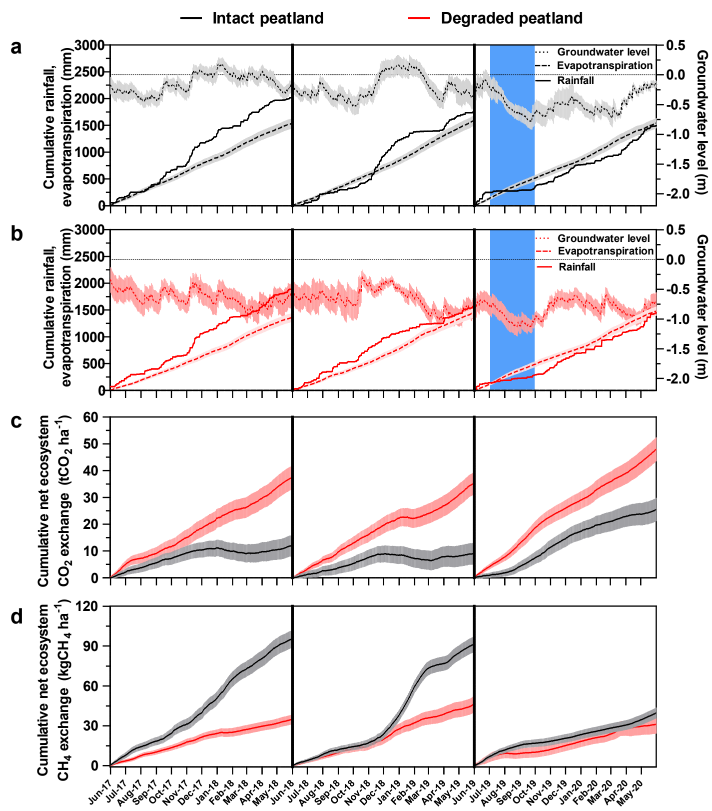

Figure 2 | Intact and degraded tropical peatland in Sumatra, Indonesia are emitting CO_2 and CH_4 to the atmosphere. Cumulative rainfall (solid line), evapotranspiration (dashed line, with cumulative uncertainty) on the left vertical axis and daily groundwater level (dotted line, with standard deviation) on the right vertical-axis at (a) the intact peatland (black) and (b) the degraded peatland (red) for three years (June 2017–May 2020). The blue shaded area shows a convergence of El-Niño and positive Indian Ocean Dipole. Hourly groundwater level were averaged from two locations around the degraded tower site and three locations in the intact peatland. Positive and negative value of groundwater level indicates water level above and below the peat surface, respectively. Rainfall variation controls groundwater level fluctuation. Annual cumulative net ecosystem (c) CO_2 and (d) CH_4 exchanges with cumulative flux uncertainty.

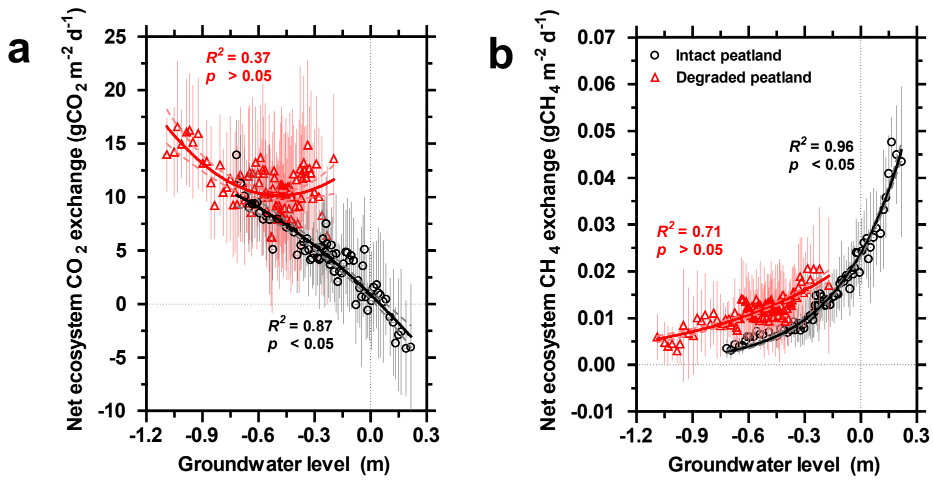

Figure 3 | The groundwater level is a key driver of both net ecosystem exchange of CO_2 and CH_4. Response of gap-filled daily (a) net ecosystem CO_2 exchanges and (b) net ecosystem CH_4 exchanges to the groundwater level at the intact (black) and degraded peatland (red). Data were binned by subgroups of 15 days values of independent variable and corresponding groundwater level and then averaged for the subgroup. The vertical bars represent the standard deviation for the subgroup. The statistical test used a significance level of 5%.

Extended Data Table 1 | Characteristics of the intact and the degraded peatland sites in Sumatra, Indonesia. Value represents average with standard deviation.

Parameter	Intact peatland	Degraded peatland	Method
Tower location	Latitude: 0° 23' 42.735" N Longitude: 102° 45' 52.382" E	Latitude: 0° 41' 58.169" N Longitude: 102° 47' 35.898" E	
Tower height (m)	48	40	
Average Canopy height (m)	32 ± 6	19 ± 6	Permanent sampling plot
Dominant understory species	*Nepenthes spp., Pandanus spp., Cyrtostachys renda*	*Dicranopteris linearis*, *Nepenthes spp., Pandanus spp., Cyrtostachys renda, Nephrolepis sp., Stenochlaena sp.*, *Blechnum sp.*	Permanent sampling plot
Dominant overstory species	*Shorea uliginosa, Calophyllum ferrugineum, Syzygium spp., Campnosperma macrophylla, Tetramerista glabra, Palaquium burckii*	*Syzygium claviflorum, Shorea teysmanniana, Stemonurus secundiflorus, Blumeodendron kurzii, Horsfieldia crassifolia*, *Macaranga pruinosa*	Permanent sampling plot
Surface peat type (0 – 0.5 m)	Fibric	Fibric	Von Post's scale for peat humification
Peat depth (m)	9.0 ± 1.0	8.4 ± 0.6	Manual subsidence pole
Surface peat bulk density (0 – 0.5 m) (g cm^{-3})	0.08 ± 0.03	0.09 ± 0.03	Gravimetric method
Carbon concentration (%) (0 – 0.5 m)	50.2 ± 2.0	55.4 ± 0.5	Loss on Ignition method
Total Nitrogen concentration (%) (0 – 0.5 m)	1.3 ± 0.2	1.5 ± 0.3	Kjeldahl method
Nitrate (ppm) (0 – 0.5 m)	1167 ± 509	1588 ± 725	Titration method
Ammonium (ppm) (0 – 0.5 m)	475 ± 130	654 ± 184	Titration method

Extended Data Table 2 | Annual average with standard deviation of environmental variables at the intact and the degraded peatland in Sumatra, Indonesia. Groundwater level were averaged from four locations around the degraded tower site and nine locations in the intact peatland. Annual peat subsidence were derived from eight locations in the intact peatland from December 2017-June 2020 and four locations around the degraded tower site from December 2016-September 2020.

	Intact peatland			Degraded peatland			
	June 2017 - May 2018	June 2018 - May 2019	June 2019 - May 2020	Oct 2016 - Sep 2017	Oct 2017 - Sep 2018	Oct 2018 - Sep 2019	Oct 2019 - Sep 2020
Photosynthetic photon flux density (μmol m^{-2} s^{-1})	680 ± 177	667 ± 170	644 ± 164	748 ± 200	727 ± 191	717 ± 183	729 ± 194
Air temperature (°C)	26.6 ± 0.9	26.9 ± 0.9	27.0 ± 0.9	26.8 ± 0.9	26.7 ± 0.9	27.2 ± 0.9	28.1 ± 1.3
Vapor pressure deficit (hPa)	7.3 ± 2.8	7.4 ± 2.8	7.2 ± 2.8	7.4 ± 2.9	7.2 ± 2.8	7.5 ± 3.0	8.0 ± 3.1
Soil temperature at 0.15 m below peat surface (°C)	27.2 ± 0.5	27.4 ± 0.1	28.1 ± 0.1				
Soil temperature at 1.5 m below peat surface (°C)	26.2 ± 0.2	25.7 ± 0.1	25.7 ± 0.1	28.4 ± 0.3	27.7 ± 0.2	27.2 ± 0.1	27.5 ± 0.1
Cumulative rainfall (mm)	2020	1756	1496	2142	1837	1325	1763
Cumulative evapotranspiration (mm)	1575	1617	1575	1372	1371	1539	1496
Groundwater level (m)	-0.15 ± 0.16	-0.21 ± 0.20	-0.47 ± 0.18	-0.51 ± 0.13	-0.67 ± 0.10	-0.74 ± 0.23	-0.73 ± 0.14
Subsidence rate (cm yr^{-1})		3.3 ± 0.7			4.2 ± 1.3		

Extended Data Table 3 | Annual net ecosystem CO_2, CH_4 and H_2O (evapotranspiration) exchanges at the intact and the degraded peatland in Sumatra, Indonesia. Table shows annual estimates from different gap-filling approaches with uncertainties associated with random error in measurements, friction velocity quality-control criteria and gap-filling approach. The bold values represent the average with standard deviation from different approaches.

	Intact peatland			Degraded peatland			
	June 2017-May 2018	June 2018-May 2019	June 2019-May 2020	Oct 2016-Sep 2017	Oct 2017-Sep 2018	Oct 2018-Sep 2019	Oct 2019-Sep 2020
Net ecosystem CO_2 exchange (tCO_2 ha^{-1} yr^{-1})							
Marginal distribution sampling	14.9 ± 5.5	8.8 ± 5.5	25.8 ± 6.2	42.2 ± 6.5	42.3 ± 6.4	46.1 ± 6.4	48.3 ± 7.0
Random forest	10.8 ± 2.2	9.2 ± 2.3	25.5 ± 2.3	35.4 ± 2.5	38.7 ± 2.1	40.4 ± 2.0	41.8 ± 1.7
Artificial neural network	10.0 ± 2.4	9.3 ± 2.4	25.6 ± 2.6	31.2 ± 2.3	35.1 ± 2.4	36.3 ± 2.5	39.3 ± 2.2
Average	**11.9 ± 3.7**	**9.1 ± 3.7**	**25.6 ± 4.1**	**36.3 ± 4.2**	**38.7 ± 4.1**	**40.9 ± 4.1**	**43.1 ± 4.4**
Net ecosystem CH_4 exchange (kg CH_4 ha^{-1} yr^{-1})							
Marginal distribution sampling	89.7 ± 6.7	86.1 ± 5.8	35.1 ± 3.7	55.1 ± 4.0	34.2 ± 3.6	43.8 ± 6.6	29.5 ± 6.6
Mean Diurnal Course	95.3 ± 6.4	91.4 ± 5.6	39.9 ± 3.8	57.3 ± 3.8	40.2 ± 3.6	45.2 ± 6.6	34.6 ± 6.6
Average	**92.5 ± 6.5**	**88.8 ± 5.7**	**37.5 ± 3.8**	**56.2 ± 3.9**	**37.2 ± 3.6**	**44.5 ± 6.6**	**32.1 ± 6.6**
Evapotranspiration (mm yr^{-1})							
Marginal distribution sampling	1520 ± 87	1537 ± 87	1522 ± 86	1263 ± 75	1439 ± 80	1485 ± 86	1398 ± 77
Random forest	1524 ± 91	1630 ± 95	1557 ± 93	1439 ± 78	1482 ± 79	1614 ± 87	1471 ± 76
Artificial neural network	1568 ± 91	1610 ± 91	1563 ± 88	1414 ± 84	1191 ± 73	1519 ± 88	1619 ± 85
Average	**1537 ± 90**	**1592 ± 91**	**1547 ± 89**	**1372 ± 79**	**1371 ± 77**	**1539 ± 87**	**1496 ± 80**

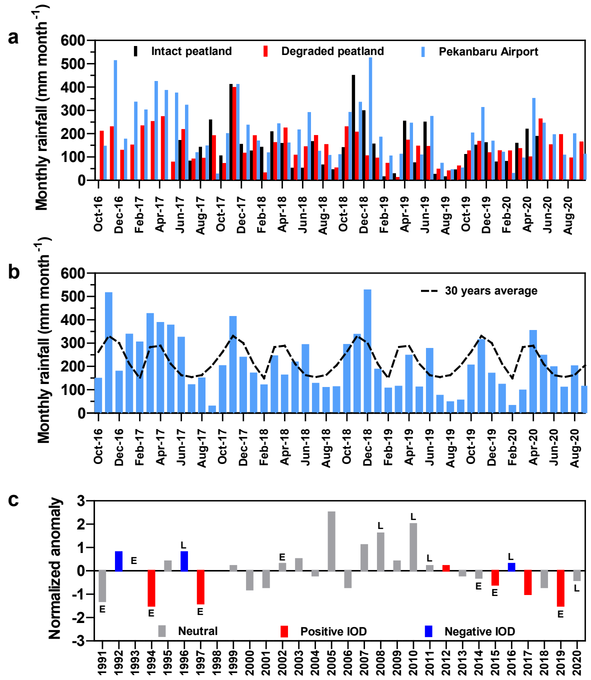

Extended Data Figure 1 | Rainfall and climate indices in the study area. (a) Comparison between monthly rainfall in the intact peatland, the degraded peatland, and Pekanbaru Airport (Riau, Sumatra) which represent the closest available long-term rainfall measurements in the region, (b) comparison between rainfall in Pekanbaru Airport during study period and long-term average of 30 years from 1991-2020 and (c) the relationship between rainfall in Pekanbaru Airport and climate indices represented with normalized anomaly of rainfall amount in July-August-September; “E” and “L” indicate El Niño and La Niña years, respectively; red and blue bars indicate positive and negative IOD years, respectively; grey bar shows neutral years. The Dipole Mode Index data were obtained from http://psl.noaa.gov/. Southern Oscillation Index were obtained from https://www.cpc.ncep.noaa.gov/data/indices/soi. The extended dry period in July-September 2019 coincided with a convergence of El-Niño and positive Indian Ocean Dipole.

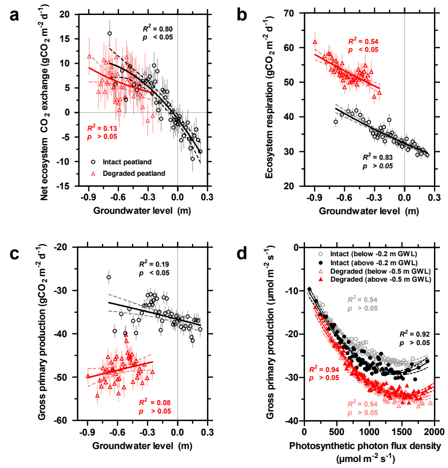

Extended Data Figure 2 | Groundwater level controls net ecosystem CO_2 exchanges. Response of (a) measured half-hourly net ecosystem CO_2 exchanges, (b) ecosystem respiration and (c) gross primary production to the groundwater level at the intact peatland (black) and the degraded peatland (red). Measured half-hourly data were grouped into daytime (06:00-18:00 hr) and nightime (18:00-06:00 hr). Then each dataset were sorted into 50 classes of groundwater level and averaged for each class. Subsequently, the daily value was computed from the average of daytime and nighttime values. The vertical bars represent the standard deviation for each class. (d) Response of the 09:00-15:00 hr gross primary production to photosyntheic photon flux density at two different groundwater level classes based on median value. The selection of time window may have created biases in actual response curves of both ecosystems, but this bias would not change the interpretation. Data were binned by subgroups of 100 half-hourly values of gross primary production and corresponding photosynthetic photon flux density and then averaged for each class. All statistical tests used a significance level of 5%. Intact peatland shows higher light-use efficiency when groundwater level is shallow.

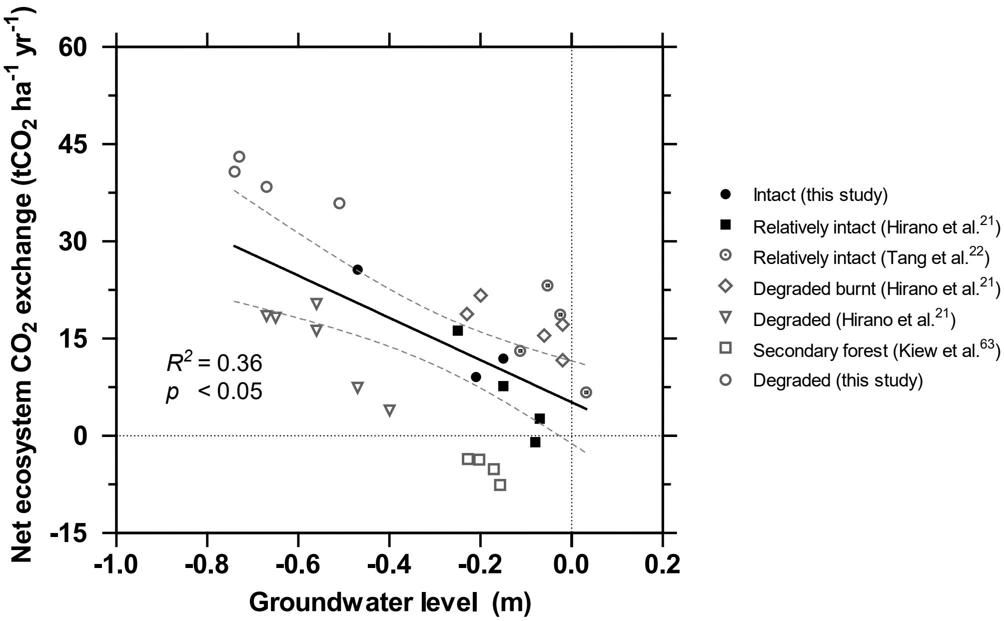

Extended Data Figure 3 | Relationship between net ecosystem CO_2 exchange and groundwater level. Data are derived from 30 site-years of the eddy covariance measurements in tropical peatlands in Southeast Asia. Solid line indicates linear relation with dashed lines for 95% confidence interval. The statistical test used a significance level of 5%. Carbon dioxide emissions increase with lower groundwater level.

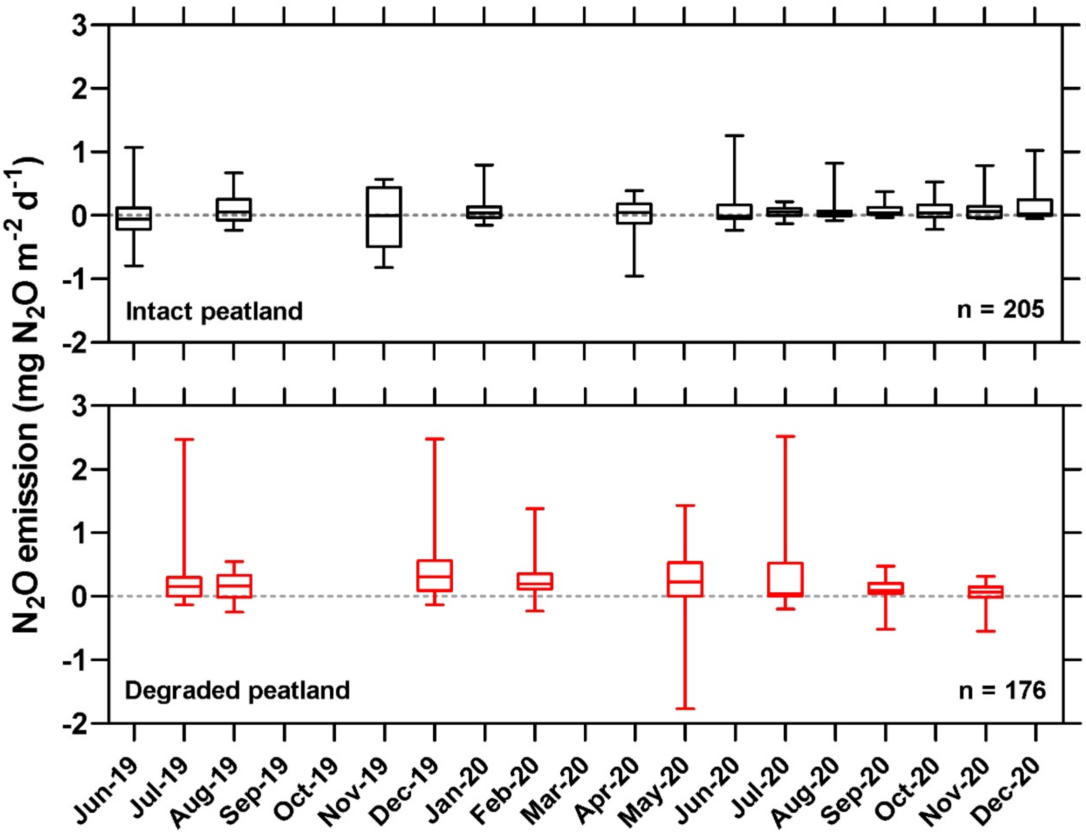

Extended Data Figure 4 | The intact peatland emits lower soil N_2O emissions than the degraded peatland. Measurements of N_2O emissions at the intact peatland (black) and the degraded peatland (red). The boxes show the median value and the interquartile range, and whiskers denote the full range of all chambers. The n values represent total number of soil N_2O flux measurements.

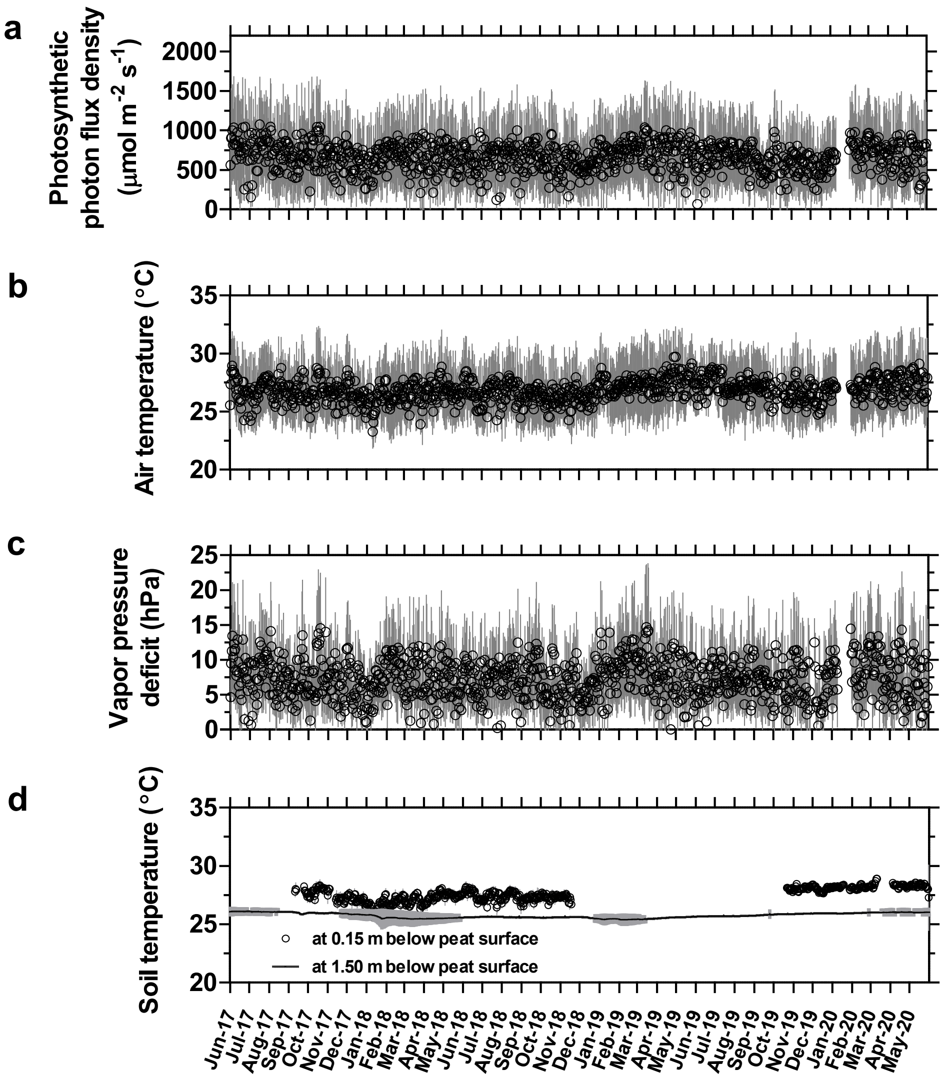

Extended Data Figure 5 | The environmental variables at the intact peatland during the study period. Variations in daily (a) photosynthetic photon flux density, (b) air temperature, (c) vapor pressure deficit and (d) soil temperature at the intact peatland. The vertical bar represents standard deviation.

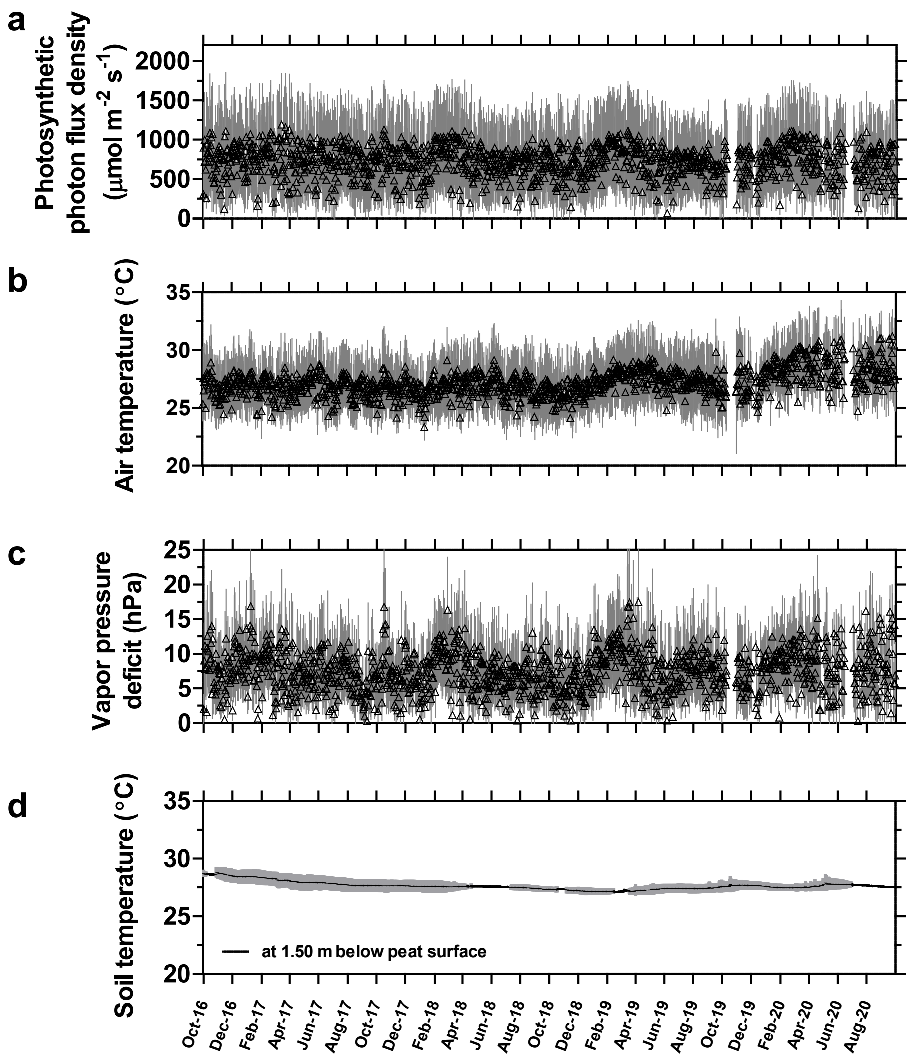

Extended Data Figure 6 | The environmental variables at the degraded peatland during the study period. Variations in daily (a) photosynthetic photon flux density, (b) air temperature, (c) vapor pressure deficit and (d) soil temperature at the degraded peatland. The vertical bar represents standard deviation.